

Understanding and Revamping of Industrial Scale SMB Units for p-Xylene Separation

Mirjana Minceva and Alirio E. Rodrigues

Laboratory of Separation and Reaction Engineering (LSRE), Dept. of Chemical Engineering, Faculty of Engineering,
Univ. of Porto, Rua Dr. Roberto Frias s/n, 4200-465 Porto, Portugal

DOI 10.1002/aic.11062

Published online November 30, 2006 in Wiley InterScience (www.interscience.wiley.com).

One of the first applications of Simulated Moving Bed (SMB) technology was in p-xylene recovery from mixed xylenes. The three main industrial processes for p-xylene separation from mixed xylenes based on SMB technology are: UOP's Parex, IFP's Eluxyl, and Toray's Aromax. These units operate in liquid phase ($T = 180^{\circ}\text{C}$ and $P = 9$ bar), achieving high recovery of almost pure p-xylene with high on-stream efficiency and extended adsorbent life. In this work, the industrial scale SMB process is investigated from modeling, simulation, and optimization points of view, using experimentally measured xylene adsorption equilibrium and kinetics data on ion exchanged faujasite zeolite. The aim is to develop tools for training of SMB unit operators and choice of the best operating conditions. Useful studies for better understanding of the influence of the operating parameters, adsorbent packing, and separation requirements on unit productivity are presented. SMB unit revamping strategies and operative actions are proposed. The practical application of "separation volume" methodology in the selection of optimum operating conditions that lead to maximum p-xylene productivity with minimal desorbent consumption is described. © 2006 American Institute of Chemical Engineers AIChE J, 53: 138–149, 2007

Keywords: Simulated Moving Bed, p-xylene, unit revamping, separation volume optimization

Introduction

The feedstocks used for xylene production (catalytic reformate, pyrolysis gasoline, and toluene disproportionation) contain a mixture of xylene isomers and ethylbenzene. The p-xylene is the one with major industrial importance since it is used as a raw material in the manufacture of polyethylene terephthalate (PET), used in production of polyester fibers, molded plastics, films, and blown beverage bottles. The separation of the p-xylene isomer from mixed xylenes is a classical issue in the petrochemical industry. The fractional distillation could be applied for o-xylene and eventually for ethylbenzene separation, but not for p-xylene separation,

because its boiling point is too close to that of m-xylene. Hence, the differences in xylenes' freezing points and adsorption characteristics are exploited commercially. Basically, there are two methods currently used to separate high purity p-xylene from a mixture of xylenes: crystallization and adsorption. Recently, a new hybrid crystallization/adsorption process has been successfully field-demonstrated.¹ Currently, about 40% of the p-xylene produced worldwide is by crystallization technology and 60% by adsorption technology.

The separation of p-xylene by adsorption uses Simulated Moving Bed (SMB) technology. SMB is a continuous chromatographic countercurrent process developed in the 1960s by Universal Oil Products.² The SMB unit consists of a set of columns connected in series; the countercurrent flow of solid and liquid phases is simulated by the periodic shifting of inlet (feed and desorbent) and outlet (extract and raffinate) streams in the direction of the fluid flow. Separation is

Correspondence concerning this article should be addressed to A. E. Rodrigues at arodrig@fe.up.pt.

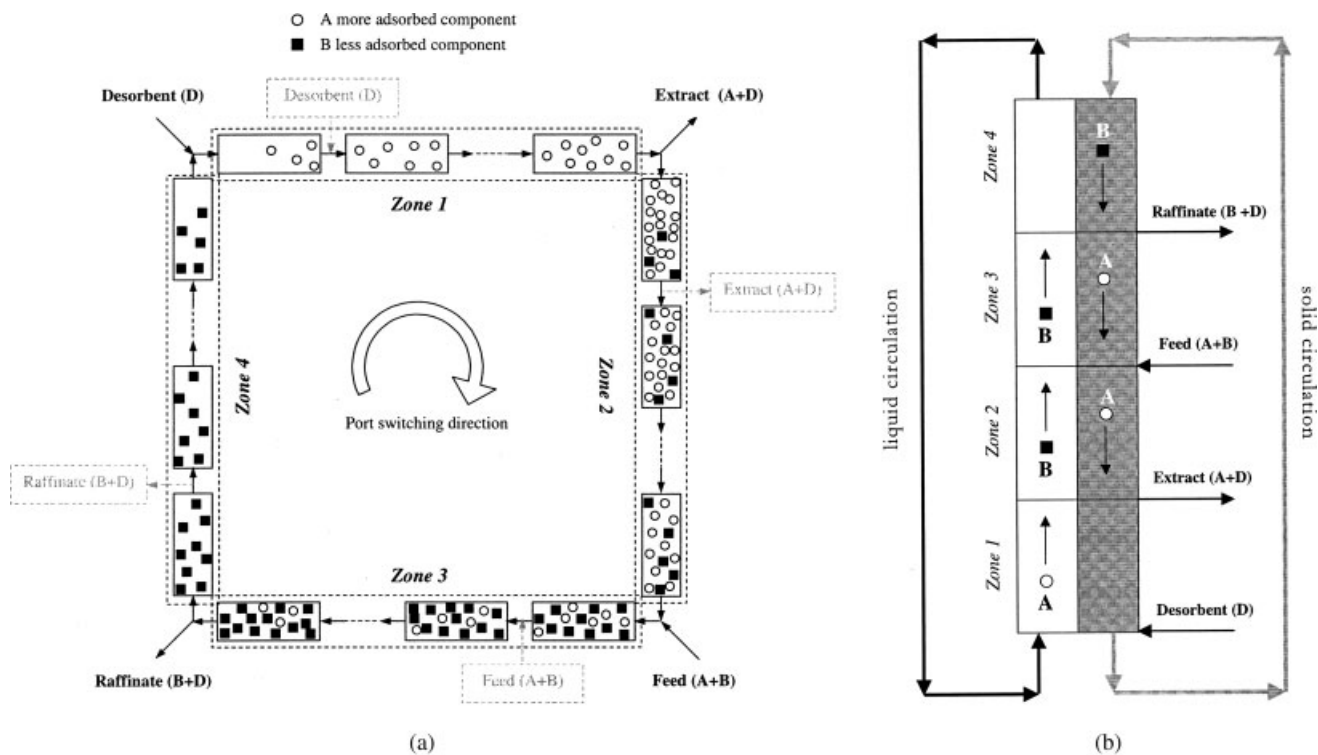


Figure 2. Schematic diagram of: (a) SMB and (b) TMB unit.

switching time as well as column length. In a previous work,¹⁹ it was confirmed that the performance of industrial scale SMB units (24 columns) for p-xylene separation can be reasonably predicted with the equivalent TMB modeling strategy. The main reason for modeling of an equivalent TMB unit instead of the real SMB unit lies in the different level of difficulty involved in the solution of the two models and the required time for their computation. TMB operates in steady state, and its stationary behavior can be described by a set of ordinary differential and algebraic equations.

In this work, a general mathematical model is used to describe an industrial scale SMB unit for p-xylene separation from a mixed xylenes stream. This model can be extended for each particular process (Parex, Eluxyl, and Aromax) in order to include the unit characteristics in terms of transfer lines, distributors, pump around tubing, flushing streams, and valve/valves configuration and operation.

The steady state equivalent TMB model considers axial dispersion flow for the liquid phase and plug flow for the solid phase, linear driving force (LDF) for the intraparticle mass transfer rate, and multicomponent adsorption equilibria described by the Langmuir isotherm. The mathematical model assumes that there is no contamination of any stream due to the transfer line dead volume.

The model equations are:

Mass balance in a volume element of zone j :

$$\varepsilon D_{Lj} \frac{d^2 c_{ij}}{dz^2} - \varepsilon v_j \frac{dc_{ij}}{dz} - (1 - \varepsilon) k_{Li} (c_{ij} - \bar{c}_{p_{ij}}) = 0 \quad (1)$$

Particle mass balance:

$$u_s \left(\varepsilon_p \frac{d\bar{c}_{p_{ij}}}{dz} + \rho_p \frac{dq_{ij}}{dz} \right) + k_{Li} (c_{ij} - \bar{c}_{p_{ij}}) = 0 \quad (2)$$

$$\frac{1}{k_{Li}} = \frac{1}{k_{fi}} + \frac{1}{\varepsilon_p k_{pi}} \quad (3)$$

$$k_{pi} = \frac{5D_{mi}/\tau}{r_p} \quad (4)$$

$$k_{fi} = \frac{Sh_p d_p}{D_{mi}} \quad (5)$$

$$Sh_p = \frac{1.09}{\varepsilon} (Re_p Sc)^{0.33} \quad (6)$$

where k_{Li} is the global mass transfer coefficient; k_{fi} is the external mass transfer coefficient; k_{pi} is the internal mass transfer coefficient; D_{mi} is the molecular diffusion; τ is tortuosity; d_p is the particle diameter; ε is the bed porosity; Sh_p and Re_p are, respectively, the Sherwood and Reynolds numbers, relative to the particle; and Sc is the Schmidt number.

Adsorption equilibrium isotherm:

$$q_{ij}^* = \frac{q_{mi} K_i \bar{c}_{p_{ij}}}{1 + \sum_{i=1}^{N_i} K_i \bar{c}_{p_{ij}}} \quad (7)$$

Boundary conditions:

$$z = 0; c_{ij}^{in} = c_{ij} - \frac{D_{Lj}}{v_j} \frac{dc_{ij}}{dz} \quad \text{and} \quad z = L; \frac{dc_{ij}}{dz} = 0 \quad (8)$$

$$\begin{aligned} \bar{c}_{p_{ij},L_j} &= \bar{c}_{p_{ij},-1.0} \quad \text{for } j = 1 \dots 23 \\ \bar{c}_{p_{ij},L_j} &= \bar{c}_{p_{ij},0} \quad \text{for } j = 24 \end{aligned} \quad (9)$$

where i is the number of the components $i = PX, MX, OX, EB, p - DEB$; j is the number of the zones $j = 1, 2, 3, 4$; c_{ij} and $\bar{c}_{p_{ij}}$ are the bulk fluid phase and average pore concentrations; q_{ij}^* is the adsorbed phase concentration in equilibrium with $\bar{c}_{p_{ij}}$; D_{Lj} is the axial dispersion coefficient; ε is the bed porosity; ε_p is the particle porosity; v_j and u_s are the liquid phase and solid phase interstitial velocities; and z is the axial coordinate. Balances at the nodes of the inlet and outlet lines of the TMB are:

Desorbent node:

$$Q_4 + Q_D = Q_1 \quad c_{i,4}^{out} Q_4 + c_{i,D} Q_D = c_{i,1}^{in} Q_1 \quad (10)$$

Extract node:

$$Q_1 - Q_X = Q_2 \quad c_{i,1}^{out} = c_{i,2}^{in} = c_{i,X} \quad (11)$$

Feed node:

$$Q_2 + Q_F = Q_3 \quad c_{i,2}^{out} Q_2 + c_{i,F} Q_F = c_{i,3}^{in} Q_3 \quad (12)$$

Raffinate node:

$$Q_3 - Q_R = Q_4 \quad c_{i,3}^{out} = c_{i,4}^{in} = c_{i,R} \quad (13)$$

The model equations were numerically solved by gPROMS.^{23,24} The mathematical model is a system of ordinary differential and algebraic equations (DAE). The axial domain is discretized using a third order orthogonal collocation method in finite elements (OCFEM) over eight elements per column. The resulting system of algebraic equations (AE) was solved by BDNLSOL solver ("Block Decomposition NonLinear SOLver") incorporated in gPROMS. For a typical simulation, CPU times of about 6 sec are required on a Pentium IV 2300 MHz processor with 2 GB RAM memory.

SMB performance

The SMB operation is evaluated through the following performances:

p-xylene purity (%)

$$PUX = \frac{c_X^{PX}}{(c_X^{PX} + c_X^{MX} + c_X^{OX} + c_X^{EB})} \times 100 \quad (14)$$

p-xylene recovery (%)

$$REX = \frac{c_X^{PX} Q_X}{c_X^{PX} Q_F} \times 100 \quad (15)$$

Productivity (kg/m³ h)

$$PR = \frac{Q_X c_{PX,X}}{V_{ads}} \quad (16)$$

Desorbent consumption (m³/kg)

$$DC = \frac{Q_D}{Q_F c_{PX,F}} \quad (17)$$

SMB design

The successful design and operation of an existing SMB unit depends upon the correct selection of operating conditions and, in particular, of the flow-rates in each zone and the switching time, that is, solid phase velocity. Design tools, such as "triangle theory"²⁵ and "separation volume"²⁶ methodology, are useful tools for a priori selection of possible operating conditions for achievement of the separation requirement. In both, the operating conditions are expressed in terms of γ_j values, the ratio between the liquid and solid interstitial velocities in each zone:

$$\gamma_j = \frac{v_j}{u_s} \quad (18)$$

which are directly linked to the SMB operating conditions with the following correlations:

$$v_j = v_j^{SMB} - u_s \quad \text{and} \quad u_s = \frac{L_c}{t^*} \quad (19)$$

where u_s is the equivalent TMB interstitial solid velocity, L_c is the SMB column length, t^* is the SMB switching time period, v_j is the TMB interstitial liquid velocity, and v_j^{SMB} is the SMB interstitial fluid velocity.

Some constraints have to be met in order to recover the p-xylene (A) in the extract and the rest of the C₈ aromatics (B) in the raffinate. These constraints are expressed in terms of net fluxes of components in each zone. In zone 1 the p-xylene must move upward in the liquid phase to the extract port; in zones 2 and 3 the p-xylene must move downward in the solid phase to the extract port and the o-, m-xylene, and ethylbenzene must move with the liquid to the raffinate port; and in zone 4 the net flux of the o-, m-xylene, and ethylbenzene has to be downwards (see Figure 2b). The net flow constraints equations in each zone are:

Zone 1:

$$\gamma_1 \frac{\varepsilon}{(1 - \varepsilon)} \frac{c_{PX1}}{\rho_p q_{PX1}} > 1 \quad (20)$$

Zone 2:

$$\gamma_2 \frac{\varepsilon}{(1 - \varepsilon)} \frac{c_{PX2}}{\rho_p q_{PX2}} < 1 \quad \gamma_2 \frac{\varepsilon}{(1 - \varepsilon)} \frac{c_{MX(OX,EB)2}}{\rho_p q_{MX(OX,EB)2}} > 1 \quad (21)$$

Zone 3:

$$\gamma_3 \frac{\varepsilon}{(1 - \varepsilon)} \frac{c_{PX3}}{\rho_p q_{PX3}} < 1 \quad \gamma_3 \frac{\varepsilon}{(1 - \varepsilon)} \frac{c_{MX(OX,EB)3}}{\rho_p q_{MX(OX,EB)3}} > 1 \quad (22)$$

Zone 4:

$$\gamma_4 \frac{\varepsilon}{(1 - \varepsilon)} \frac{c_{MX(OX,EB)4}}{\rho_p q_{MX(OX,EB)4}} < 1 \quad (23)$$

In the case of SMB units for p-xylene separation from the C₈ fraction, the first priority is the production of high purity

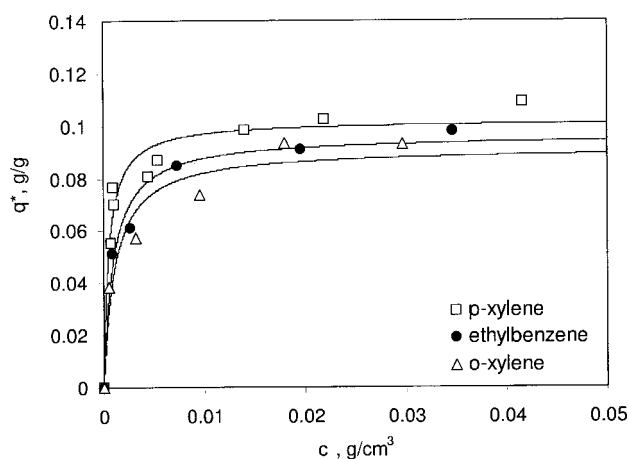


Figure 3. Adsorption equilibrium isotherms of p-xylene, ethylbenzene, and o-xylene at 180°C and 8 bar.

Symbols = experimental and lines = predicted with Langmuir model.

p-xylene, and the second priority is maximizing recovery, which in practice means a raffinate almost free of p-xylene. After adjustment of p-xylene purity and recovery, the desorbent consumption is minimized, as a third process operation priority.

When p-xylene purity drops slightly below purity requirement, the first corrective action should be done in zone 2. According to Eq. 21, to solve the problem γ_2 should be slightly increased. This can be done by increasing liquid interstitial velocity or decreasing solid interstitial velocity; the first correction is done by decreasing of the extract flow rate and the second by increasing of the switching time. Both actions will influence the other γ_j values in the same manner.

These design constraints are usually presented in a 2-D plane ($\gamma_2 \times \gamma_3$) or 3-D volume ($(\gamma_2 \times \gamma_3 \times \gamma_1)$ or $(\gamma_2 \times \gamma_3 \times \gamma_4)$). The first presentation is known as the “separation region”—the region of feasible separation is a triangle shape in a $(\gamma_2 \times \gamma_3)$ plane, with a maximum productivity for given desorbent consumption (the value of the flow rates in zones 1 and 4 are fixed a priori) in the triangle vertex. The “separation region” presentation is based on the “equilibrium theory” design concept, which for systems where mass transfer limitations are present can only give initial guesses for the feasible operating points of the process-separation region, since it is based on the assumption of the equilibrium model. The 3-D design constraints presentation, called “separation volume” methodology, offers two possibilities: (i) if the flow rate in zone 1 (γ_1) is fixed, the design leads to a $(\gamma_2 \times \gamma_3 \times \gamma_4)$ volume constructed from triangle shaped separation regions obtained for different values of γ_4 ; (ii) if the flow rate in zone 4 (γ_4) is fixed, the triangle shaped separation regions obtained for different values of γ_1 build $(\gamma_2 \times \gamma_3 \times \gamma_1)$ volume. Several vertexes are obtained, and the operating conditions $(\gamma_1, \gamma_2, \gamma_3, \gamma_4)$ leading to maximum productivity and minimum desorbent consumption would be one of these vertexes.^{21,27}

From the SMB operator’s point of view, these representations of the feasible separation regions are very useful for the location of the SMB operating conditions as a point in the separation triangle or volume. The main application is in

the location of the new operating conditions as a result of some problem arising in the process operation and fast visualization of their effect on the SMB unit performance (new operating point in or out of the separation region). They can also be used for improvement of the SMB performance, as will be shown later in this article.

Xylenes Equilibrium and Kinetics of Adsorption

The adsorption equilibrium and kinetics of single p-xylene, o-xylene, and ethylbenzene on Ba exchanged faujasite zeolite in liquid phase at 180°C and 9 bar was determined experimentally.^{14,27} The experiments were carried out in a glass jacketed 1 dm³ autoclave (Büchi, Switzerland), operating in a batch mode. For each experiment (adsorption equilibrium or kinetics), a volume of 0.35–0.4 dm³ of single xylene solution in i-octane with an initial concentration between 1 and 10 wt% was introduced in the adsorber; around 30 g of the pre-treated adsorbent was placed in a basket at the top of the stirrer shaft and the adsorber was closed and pressurized with helium. When the operating conditions ($T = 180^\circ\text{C}$ and $P = 9$ bar) were reached, the mixing was started; the basket fell down along the stirrer shaft and got in contact with the xylene/i-octane solution (time zero in the kinetics experiments). More details about the experimental set-up and experimental procedure can be found elsewhere.^{14,27}

The p-xylene, o-xylene, and ethylbenzene monocomponent adsorption equilibrium data at 180°C were fitted with the Langmuir isotherm (see Figure 3):

$$q^* = \frac{q_m Kc}{1 + Kc} \quad (24)$$

The calculated Langmuir parameters for p-xylene, o-xylene, and ethylbenzene are presented in Table 1. m-xylene has very similar adsorption equilibrium on faujasite type zeolites as o-xylene^{9,10}; therefore, m-xylene Langmuir isotherm parameters were assumed to be equal to those of o-xylene. The p-diethylbenzene was considered as desorbent. According to data from the literature,¹⁵ the *p-x/p-DEB* selectivity on Ba exchanged faujasite zeolite is around 1. The p-DEB Langmuir parameters used in the simulation are presented in Table 1.

The macropore diffusion model was used to describe the kinetics of adsorption of p-xylene, o-xylene, and ethylbenzene onto Ba exchanged faujasite adsorbent. The mathematical model is based on the following assumptions: (i) spherical bidisperse adsorbent particle with homogeneous size; (ii) negligible external mass transfer; (iii) diffusion in the macropores is rate controlling; (iv) instantaneous equilibrium between the liquid phase in the macropore and the crystals

Table 1. Langmuir Isotherm Parameters at 180°C and 9 Bar

Component	$K, \text{cm}^3/\text{g}$	$q_m, \text{g/g}$
p-xylene	1940.9	0.1024
o-xylene	888.4	0.0917
m-xylene	888.4	0.0917
ethylbenzene	1026.3	0.0966
p-deb	1902.8	0.1045

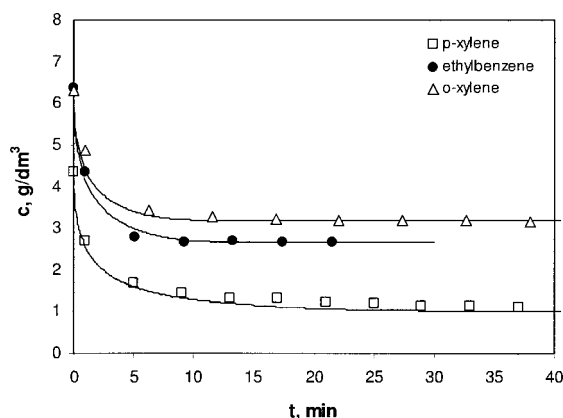


Figure 4. p-xylene, ethylbenzene, and o-xylene uptake curves at 180°C and 8 bar.

Symbols = experimental and lines = simulated with macropore diffusion model.

of Langmuir type; and (v) constant temperature. The mathematical model describes well the xylene uptake curves (see Figure 4). The results of the complete adsorption kinetics study are presented in Minceva and Rodrigues.¹⁴

Simulation of the SMB Unit

The SMB geometry, operating conditions, and model parameters are presented in Table 2. The single component Langmuir parameters, K and q_m , presented in Table 1, were used in the multicomponent Langmuir isotherm (Eq. 7). The density of the liquid mixture was considered constant, independent of mixture composition, and equal to the density of the desorbent (p-diethylbenzene), 724 kg/m³.

Influence of the switching time

The influence of the switching time on p-xylene purity and recovery was studied. Two feed flow rates were selected for this purpose: (i) low- $Q_F = 10$ m³/h and (ii) high- $Q_F = 80$ m³/h. For both cases, the operating conditions and model parameters used are those presented in Table 2. The p-xylene purity and recovery calculated for switching time between 1.06 and 1.13 are presented in Figure 5a.

When low feed flow rate is used, p-xylene purity above 99.7% and recovery above 95% can be obtained in a large

window of switching time (t^* between 1.07 and 1.12 min). This is not the case when high feed flow rate is used; the same performances can be obtained just for $t^* = 1.10$. The reason for this behavior is the location of the operating points in the separation region for $t^* = 1.10$, $PUX_{\min} = 99.7\%$, and $REX_{\min} = 90\%$, presented in the (γ_2, γ_3) plane (see Figure 5b). The separation region was constructed using the calculation algorithm, which assumes constant switching time and flow rates in zones 1 and 4, and, consequently, constant desorbent flow rate (values given in Table 2). The feed flow rate is gradually increased, starting from a very low feed flow rate. For each feed flow rate, the steady state TMB model (Eqs. 1–13) was solved for several pairs of values (γ_2, γ_3) within the region between the diagonal $\gamma_2 = \gamma_3$, the horizontal line $\gamma_3 = \gamma_4$, and the γ_3 axis. Each pair of values (γ_2, γ_3) that satisfy the extract purity and recovery criteria were selected to build the separation region. More details about the algorithm for the construction of the separation regions can be found elsewhere.¹⁹

In practice, an optimized SMB unit operates near to the vertex; the small fluctuation in the switching time could affect significantly the SMB performance. For instance, just a small decrease in the switching time ($t^* = 1.09$) will cause a drop in the extract purity to 92.4%. This operating point is marked with the circle in Figure 5b and is placed in the region where the purity constraints are valid just for the raffinate.

Construction of graphs $Purity(Recovery)$ vs. t^* for the optimized SMB unit operating conditions is very useful for prediction of the tendency of novel cyclic steady unit performances, when a variation of the switching time takes place in the unit operation.

The influence of the switching time ($t^* = 0.6, 0.7, 0.9, 1.1$, and 1.3 min) on the size and positions of the separation regions with $PUX_{\min} = 99.7\%$ and $REX_{\min} = 90\%$ is presented in Figure 6a. The liquid/solid velocity ratios in zones 1 and 4 are fixed and equal for all switching times, $\gamma_1 = 1.6$ and $\gamma_4 = 0.5$, respectively.

The separation regions become smaller with decrease of the switching time. For switching times lower than 0.5 min, the separation is not possible. The reason for this behavior is the contact time; the contact time (switching time) is not sufficiently long to ensure the mass transfer of the components from the liquid to the solid phase. The effect of the decrease of the switching time on the separation region size (reduction of its size) is similar to the effect of increase of the mass transfer resistance.

Table 2. SMB Geometry, Operating Conditions, and Model Parameters

SMB Unit Geometry		SMB Operating Conditions	
$L_c = 1$ m	$C_F^{PX} = 23.6$ wt%	$C_F^{OX} = 12.7$ wt%	
$d_c = 4$ m	$C_F^{MX} = 49.7$ wt%	$C_F^{EB} = 14.0$ wt%	
N^o , columns: 24			
Configuration: 5-9-7-3			
Model parameters	$t^* = 1.1$ min		
$\varepsilon = 0.29$ $\varepsilon_p = 0.37$			
$\rho_p = 1.48$ g/cm ³	$Q_F^{SMB} = 80.00$ m ³ /h	$Q_X^{SMB} = 87.00$ m ³ /h	
$d_p = 0.062$ cm	$Q_R^{SMB} = 241.65$ m ³ /h	$Q_D^{SMB} = 248.65$ m ³ /h	
$Pe = vL_p/D_{Lp} = 1200$	$Q_I^{SMB} = 546.81$ m ³ /h		

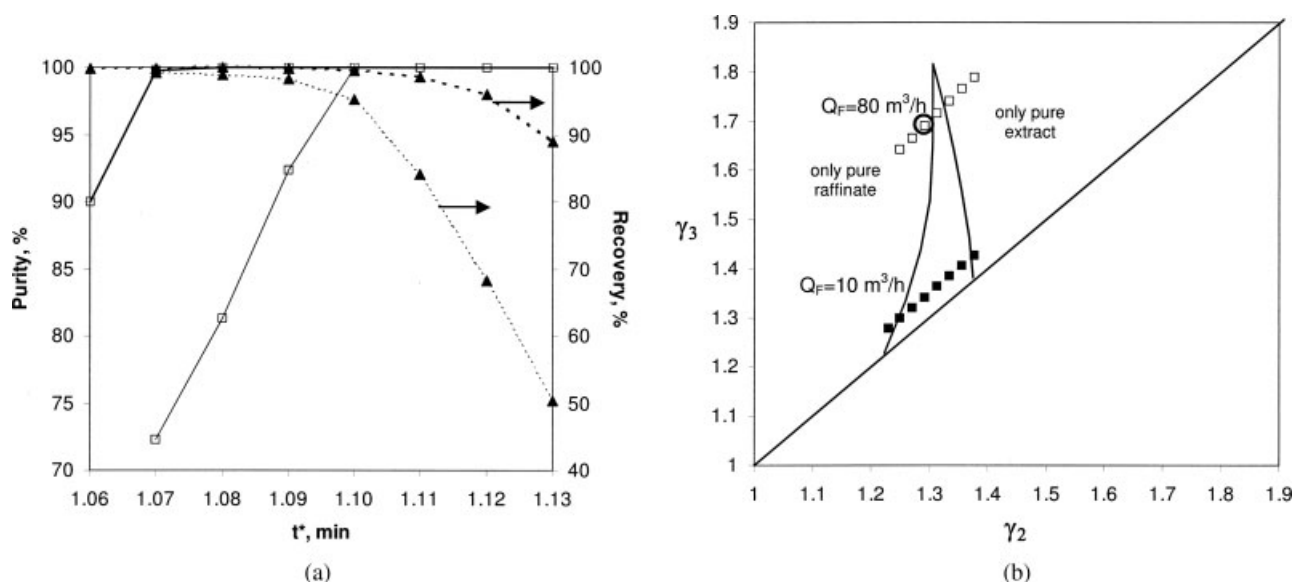


Figure 5. (a) Influence of switching time on p-xylene purity and recovery $Q_F = 10 \text{ m}^3/\text{h}$ (bold lines) and $Q_F = 80 \text{ m}^3/\text{h}$ (thin lines); (b) operating points in (γ_2, γ_3) plane for $Q_F = 10 \text{ m}^3/\text{h}$ and $Q_F = 80 \text{ m}^3/\text{h}$ (separation region for $t^* = 1.1$, $PUX_{\min} = 99.7\%$, and $REX_{\min} = 90\%$).

The separation regions expand with increase of the switching time from 0.6 min to 1.1 min; for switching time longer than 1.1 min, this enlargement becomes insignificant (see Figure 6a). Also, it is important to notice that all separation regions vertexes (connected with a gray line in Figure 6a) have the same value for γ_2 . For the chosen SMB configuration (5-9-7-3), zone 2 is long enough; and for any switching time between 0.6 min and 1.3 min, the mass transfer limitation does not affect the γ_2 value of the separation regions vertexes.

The p-xylene productivity and desorbent consumption in the vertex of the separation region for each switching time

are presented in Figure 6b. The maximum productivity is obtained for a switching time between 0.7 and 0.8 min. The desorbent consumption presented in this figure is not optimized since the γ_1 and γ_4 are fixed a priori. The optimization of the desorbent consumption is discussed later in this article.

Influence of the p-xylene recovery

The influence of the p-xylene recovery on separation regions for $t^* = 0.9 \text{ min}$, $PUX_{\min} = 99.7\%$, $\gamma_1 = 1.6$, and $\gamma_4 = 0.5$ is presented in Figure 7a. The separation regions shrink from the right side (border with only pure extract

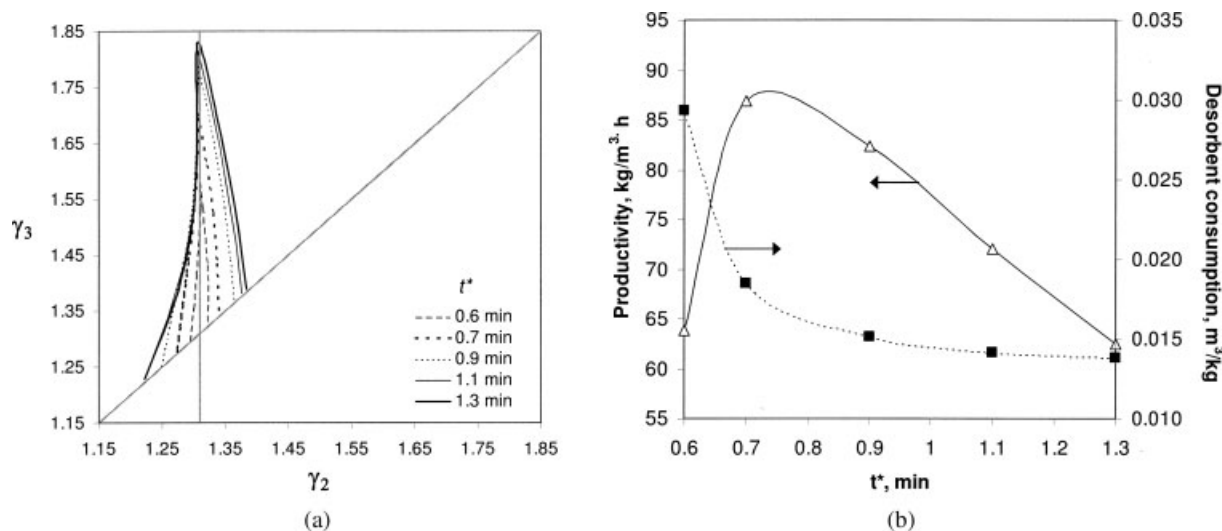


Figure 6. Influence of switching time on the (a) separation regions ($PUX_{\min} = 99.7\%$, $REX_{\min} = 90\%$, $\gamma_1 = 1.6$, and $\gamma_4 = 0.5$) and (b) p-xylene productivity and desorbent consumption in the vertex of the separation regions.

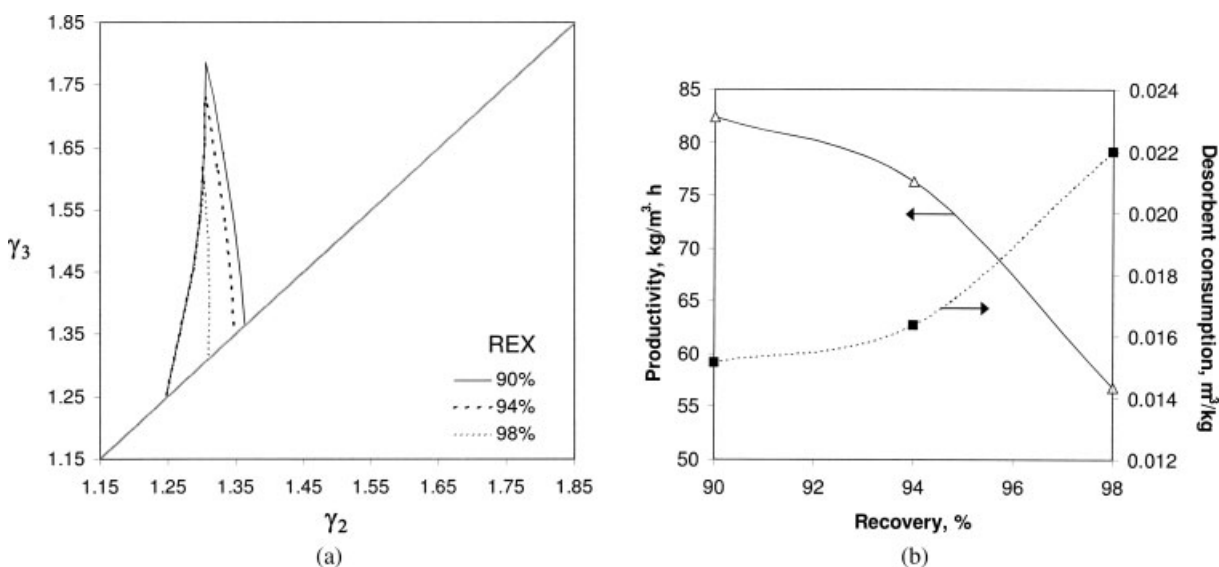


Figure 7. Influence of the required p-xylene recovery on (a) the separation region ($t^* = 0.9$ min, $PUX_{\min} = 99.7\%$, $\gamma_1 = 1.6$, and $\gamma_4 = 0.5$) and (b) p-xylene productivity and desorbent consumption in the vertex of the separation regions for $REX_{\min} = 90\%$, 94% , and 98% .

region) with the increase of the product recovery requirements from 90% to 98%; the left side border remains unchanged since the p-xylene purity requirement is kept unchanged, $PUX_{\min} = 99.7\%$. The p-xylene productivity and desorbent consumption were calculated in the vertexes of the separation regions for p-xylene recovery 90%, 94%, and 98% (see Figure 7b). The p-xylene productivity decreases around 30%, and desorbent consumption increases around 45% when the required p-xylene recovery increases from 90% to 98%. It could be acceptable to operate the unit with 90% p-xylene recovery, since the p-xylene lost in the raffinate is anyhow recycled to the process by passing through an isomerization reaction before entering again in the SMB through the feed stream.

Combined influence of switching time and recovery requirement

The combined influence of the switching time and p-xylene recovery requirement on SMB productivity was calculated using the optimization algorithm presented in Figure 8. The steady state equivalent TMB model was applied together with the adsorption equilibrium data, unit configuration, and model parameters presented in Tables 1 and 2. In the algorithm the unit geometry (column geometry and number of columns per zone), initial value of the switching time, and initial value of the feed flow rate are used as input data.

In the first step, the switching time is selected ($t^* = t_0^*$); the objective is to find the flow rates in four zones that provide the minimum desorbent consumption for given feed throughput (flow rate). The feed flow rate is increased gradually. For each feed flow rate, the optimum (minimum desorbent consumption) within the optimization constraints (minimum p-xylene recovery and purity) is found. The optimization is carried on until the feed flow rate for which a feasible minimum exists. This feed flow rate is the maximum that can be processed in the SMB unit within the specified p-xy-

lene recovery and purity. In the second step, the switching time is increased ($t^* = t_0^* + p\Delta t$) and step one is repeated. The calculation stops when the final switching time defined by the user is reached ($t^* = 1.0$ min).

The productivity calculated with the maximum feasible feed flow rate obtained for each switching time is used to construct the productivity versus switching time curves presented in Figure 9a. The p-xylene purity requirement is set to 99.7%. The optimization is run for three different values of

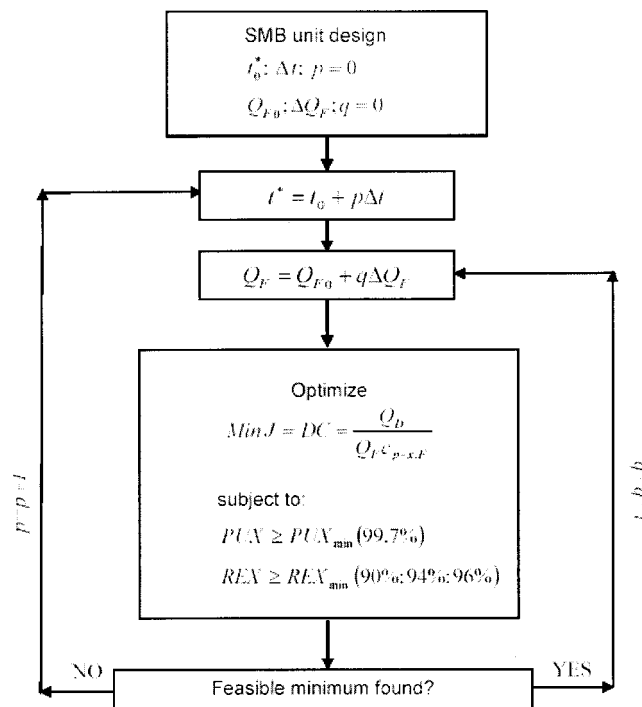


Figure 8. Flow sheet of the optimization algorithm.

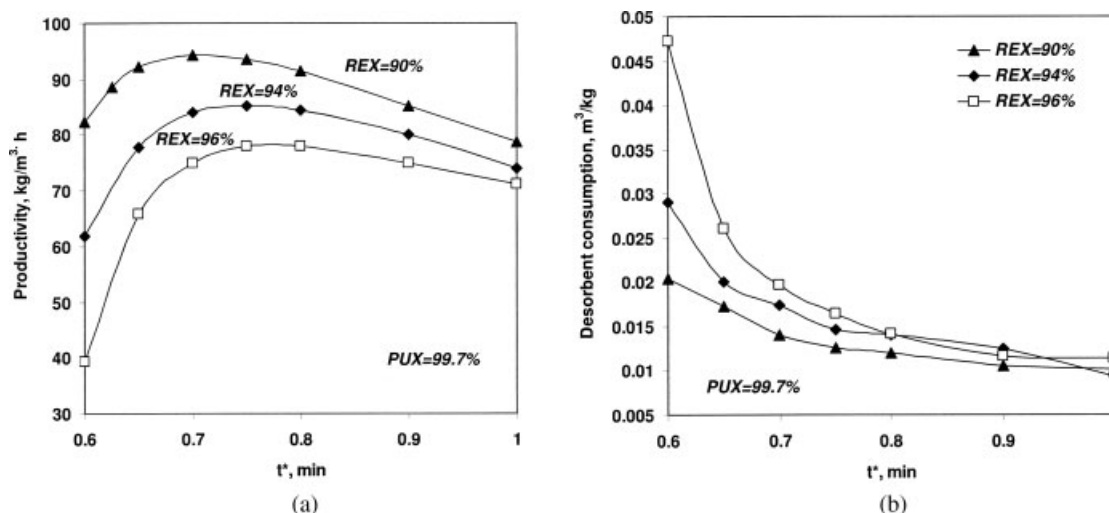


Figure 9. (a) Productivity versus switching time for paraxylene recovery $REX_{\min} = 90\%$, 94% , and 98% and extract purity $PUX_{\min} = 99.7\%$; and (b) desorbent consumption versus switching time for paraxylene recovery $REX_{\min} = 90\%$, 94% , and 98% and extract purity $PUX_{\min} = 99.7\%$.

p-xylene recovery: 90%, 94%, and 96%. Each point in Figure 9a corresponds to the optimal flow rates in all four SMB zones obtained for a given switching time, which lead to maximum p-xylene productivity with a corresponding minimum desorbent consumption needed to achieve minimal requested p-xylene recovery and purity. The minimal desorbent consumption corresponding to each point in Figure 9a is presented in Figure 9b.

The highest p-xylene productivity for $REX_{\min} = 94$ and $REX_{\min} = 96\%$ is obtained for $t^* = 0.75$ min, and for $REX_{\min} = 90\%$ at $t^* = 0.7$ min. The productivity increases from 77.94 to 94.35 $\text{kg/m}^3 \cdot \text{h}$ with release of the recovery constraints from 96% to 90%. The desorbent consumption also decreases with decrease of the p-xylene recovery requirement, from 0.0165 m^3/kg ($REX_{\min} = 96\%$, $t^* = 0.75$ min) to 0.0140 m^3/kg ($REX_{\min} = 90\%$, $t^* = 0.7$ min).

SMB unit revamping strategies

The SMB unit revamping strategies proposed here are based on the results from the study of the combined influence of the switching time and recovery requirements on SMB unit productivity. The SMB unit revamping considers the increase of the unit productivity without changing the unit geometry, configuration, and adsorbent used.

Taking into consideration Figure 9, three main conclusions can be drawn: (i) there is an optimal switching time in terms of the maximum p-xylene productivity; (ii) there is a minimum switching time (in this case, 0.5 min) below which the separation requirements are not met due to mass transfer limitation; and (iii) for a fixed switching time, SMB productivity can be increased by decreasing the p-xylene recovery requirements.

The SMB unit operating at given switching time, such as 0.9 min, and given p-xylene recovery, such as 96%, can be revamped by: (i) keeping the switching time and reducing the recovery requirement; (ii) reducing the switching time to its optimal value and keeping the p-xylene recovery

unchanged; or (iii) both, reducing the switching time to its optimal value and reducing the recovery requirement. With the first strategy, for $t^* = 0.9$ min, passing from recovery 96% to 90%, the SMB productivity will increase from 74.91 $\text{kg/m}^3 \cdot \text{h}$ to 85.13 $\text{kg/m}^3 \cdot \text{h}$. With the second revamping strategy, by decreasing switching time to its optimal value ($t^* = 0.75$ min) and keeping recovery requirement on 96%, the productivity will increase up to 77.94 $\text{kg/m}^3 \cdot \text{h}$. In the third strategy, the productivity increases from 74.91 $\text{kg/m}^3 \cdot \text{h}$ ($t^* = 0.9$ min, $REX_{\min} = 96\%$) to 94.35 $\text{kg/m}^3 \cdot \text{h}$ ($t^* = 0.7$ min, $REX_{\min} = 90\%$).

Let us see now how this applies in terms of zone operating conditions. The values of γ_j for each point in Figure 9 are presented in Figure 10. For a fixed value of p-xylene recovery, the value of γ_2 is constant over the switching time; γ_3 and γ_4 increase slightly and γ_1 decreases slightly with increase of the switching time from 0.6 min to 1 min.

After selecting the revamping strategy, the SMB operator can choose a new operating point from Figure 9 and read the corresponding γ_j from Figure 10. Then, from the selected switching time, the solid interstitial velocity can be calculated (Eq. 19) and used for estimation of the liquid interstitial velocity (liquid flow rate) by Eq. 18; at the end, the stream flow rates can be calculated using Eqs. 11–13.

From the operational point of view, the first strategy is easiest to apply; decrease of the recovery requirement under constant switching time can be simply done by increasing feed and raffinate flow rates for a same value. In this way, the values of γ_1 , γ_2 , and γ_4 are kept constant, and γ_3 to its optimal value associated to the p-xylene recovery. In the second and third strategy, besides the decrease of switching time, all internal and external liquid flow rates have to be corrected. The percentage of needed increase is different for all streams and zone flow rates. Therefore, the best operational strategy, in order to keep the p-xylene purity less affected, is to decrease the switching time gradually, followed by the needed change of inlet and outlet streams flow rates (calculated from γ_j presented in Figure 10). When apply-

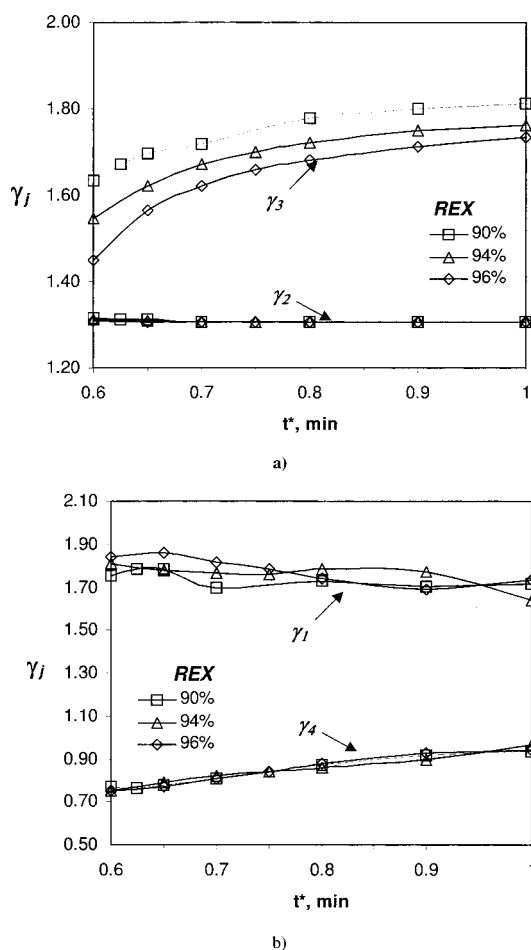


Figure 10. γ_i values corresponding to operating points presented in Figure 9: (a) γ_2 and γ_3 ; (b) γ_1 and γ_4 .

ing the third strategy, it is better first to start with (i) a gradual decrease of switching time and increase the zone flow rates in accordance to the optimal γ_i values for each switching time and then (ii) for the optimum switching time to increase the feed flow rate to its optimum value with simultaneous increase of the raffinate flow rate.

Influence of the bed capacity

The size of the adsorbent particles used in industrial SMB units for p-xylene separation vary between 0.03 cm and 0.1 cm, with a mean particle diameter around 0.06 cm. Special attention is given to packing of the industrial columns in order to get the maximum bed capacity obtained when the lowest possible bed porosity is achieved. For this purpose, specific packing tools are developed and used. It is interesting to see the influence of the bed capacity on the unit performances. This is done by studying of the effect of the porosity on the separation region size and position. The bed porosity was varied between 0.29 and 0.38 and $t^* = 0.9$ min, $PUX_{\min} = 99.7\%$, $REX_{\min} = 94\%$, $\gamma_1 = 1.6$, and $\gamma_4 = 0.5$. The regions of separation move to higher (γ_2 , γ_3) values when lower bed porosity is used (Figure 11). The productiv-

ity increases from 59.39 kg/m³h to 76.3 kg/m³ h and desorbent consumption decreases from 0.0240 m³/kg to 0.0164 m³/kg when ϵ drops from 0.38 to 0.29. Great improvement of the SMB performances could be obtained with use of the minimum possible bed porosity.

Separation volumes

The optimization of the existing SMB unit considers the choice of the operating parameters in order to obtain the maximum productivity with a minimum desorbent for a given p-xylene purity and recovery. For a fixed value of the switching time, the optimal operating point ($\gamma_1, \gamma_2, \gamma_3, \gamma_4$) could be obtained with the two-level optimization procedure.²¹ This procedure is based on the "separation volume" methodology, using a realistic mathematical model (equivalent steady state TMB, which considers the presence of external and internal mass transfer resistance), and explores the influence of the flow rates in zones 1 and 4.

In this section the influence of the flow rate in zone 1 and zone 4 on the SMB unit performances will be demonstrated. The separation volumes ($\gamma_2 \times \gamma_3 \times \gamma_1$) and ($\gamma_2 \times \gamma_3 \times \gamma_4$) for $t^* = 0.9$ min, $REX_{\min} = 94\%$, and $PUX_{\min} = 99.7\%$ are presented in Figures 12a and 12b, respectively.

In Figure 12a, for a fixed value of the flow rate in zone 4 ($\gamma_4 = 0.9$), the separation region increases by increasing γ_1 up to 1.6; further increase of γ_1 does not influence the size of the separation regions. While the size of the separation region increases, the vertex moves from lower to higher values of (γ_2 , γ_3), which means that higher feed flow rate could be processed and higher productivity could be reached ($\max(PR) = \max(Q_F) = \max(\gamma_3 - \gamma_2)$). When the separation region size does not increase more, further increment in γ_1 will not affect SMB unit productivity.

When the value of γ_1 is fixed ($\gamma_1 = 1.6$) the separation regions are of similar shape and size until $\gamma_4 = 0.9$ and then

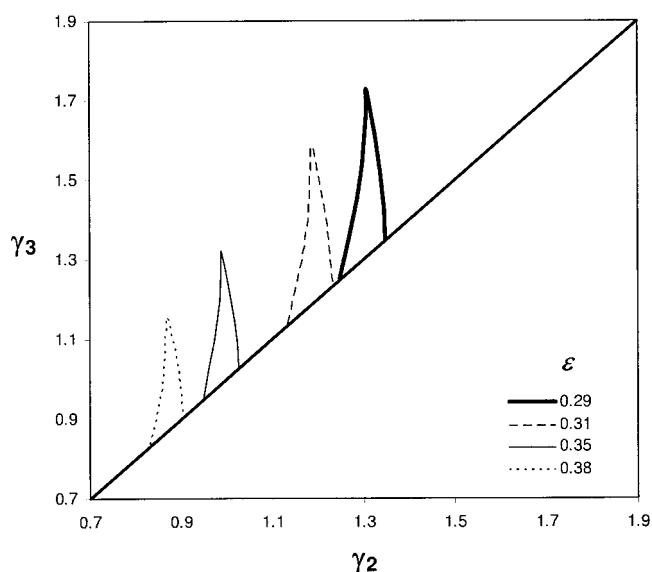


Figure 11. Influence of the bed porosity on separation regions $PUX_{\min} = 99.7\%$, $REX_{\min} = 94\%$, $\gamma_1 = 1.6$ and $\gamma_4 = 0.5$.

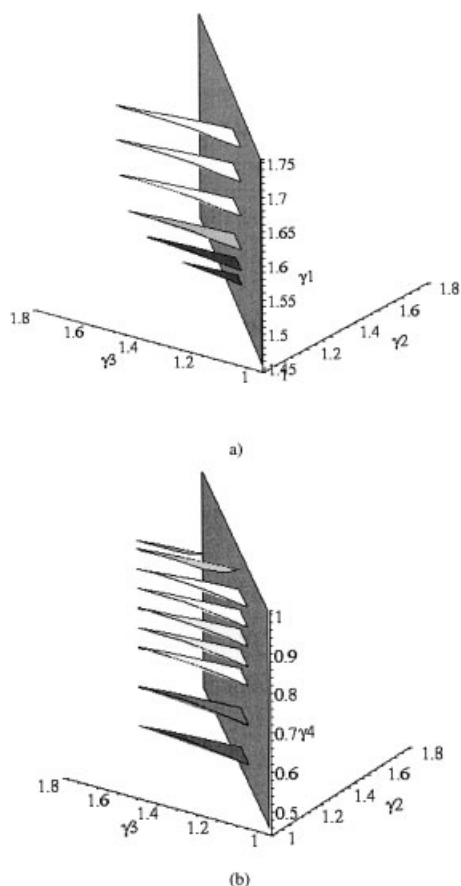


Figure 12. (a) $(\gamma_1 \times \gamma_2 \times \gamma_3)$ separation volume, for $\gamma_4 = 0.9$ and (b) $(\gamma_4 \times \gamma_2 \times \gamma_3)$ separation volume plot, for $\gamma_1 = 1.6$ ($t^* = 0.9$ min, $REX_{\min} = 94\%$ and $PUX_{\min} = 99.7\%$).

they start to decrease with further increase of the value of γ_4 (Figure 12b). The value of the flow rate in zone 4 (γ_4) does not influence the feed flow rate and SMB unit productivity, but it affects the desorbent consumption. For fixed γ_1 , it will be of interest to work with the highest possible γ_4 value in the region of unchanged separation region size, because less desorbent will be spent, since $\min(DC) = \min(Q_D) = \min(\gamma_1 - \gamma_4)$. In summary, with the above analysis, the SMB operator can foresee the optimum operating point for $t^* = 0.9$ min, $REX_{\min} = 94\%$, and $PUX_{\min} = 99.7\%$, which is expected around $\gamma_1 = 1.6$, $\gamma_2 = 1.31$, $\gamma_3 = 1.75$, and $\gamma_4 = 0.9$. For precise determination of the optimal operating point, the use of the “two-level optimization procedure”²¹ is needed.

Conclusions

The most important aspects in operation of an industrial scale SMB unit for p-xylene separation from the C_8 fraction are presented. Useful tools for process understanding, operation, and optimization, aimed to help SMB process operators, are presented.

The SMB process is investigated from modeling, simulation, and optimization points of view, using experimentally determined xylene adsorption equilibrium and kinetics data

on ion exchanged faujasite zeolite. The influence of the operating parameters, bed porosity, and separation requirements on the unit productivity was presented. The study of the effect of the bed capacity has shown that SMB productivity can be significantly improved when the unit operates at minimal possible bed porosity.

The algorithm used for optimization of the SMB unit, taking into account the mutual influence of the switching time and p-xylene recovery requirements, results in three SMB revamping strategies and corresponding operative actions.

The practical application of “separation volume” methodology in visualization of the constraints in the SMB unit zones flow rates, as well as good starting points in selection of optimum operating conditions that lead to maximum p-xylene productivity with minimal desorbent consumption, is described.

Acknowledgments

This work was financially supported by the project POCTI/EQU/44515/2002 (Fundação para a Ciência e Tecnologia—FCT). Mirjana Minceva gratefully acknowledges the FCT post-doctoral grant SFRH/BPD/19733/2004/1736.

Literature Cited

1. *Eluxyl Simulated Countercurrent Adsorption of Paraxylene*. IFP Industrial Division brochure. Paris, France; 1998.
2. Broughton DB, Gerhold CG. *Continuous Sorption Process Employing Fixed Bed of Sorbent and Moving Inlets and Outlets*. U.S. Patent No. 2 985 589; 1961.
3. Broughton DB, Neuzil RW, Pharis JM, Brearley CS. The Parex process for recovering paraxylene. *Chem Eng Prog*. 1970;66:70–75.
4. Otani S, Akita S, Iwamura T, Kanaoka M, Matsumura K, Noguchi Y, Sando K, Mori T, Takeuchi I, Tsuchiya T, Yamamoto T. *Separation Process of Components of Feed Mixture Utilizing Solid Sorbent*. U.S. Patent No. 3 761 533; 1973.
5. Ash G, Barth K, Hotier G, Mank L, Renard P. Eluxyl: a new paraxylene separation process. *Revue de l'Institut Français du Pétrole*. 1994;49:541–549.
6. Purse FV, Carson DB. *Rotary Valve*. U.S. Patent No. 3 040 777; 1962.
7. Hotier G, Roux GC, Nguyen TT. *Process for Separation of p-Xylene in C8 Aromatic Hydrocarbons with a Simulated Moving Bed Adsorption and Crystallization*. U.S. Patent No. 5 922 924; 1999.
8. Otani S. Adsorption separates xylenes. *Chem Eng*. 1973;80:106–107.
9. Neves SB. Modeling of Adsorption Fixed-Bed in Liquid-Solid Systems. M.Sc. Thesis, Universidade Federal da Bahia, Brazil; 1995.
10. Santacesaria E, Morbidelli M, Danise P, Mercenari M, Carra S. Separation of xylenes on y zeolite. 1. Determination of the adsorption equilibrium parameters, selectivities and mass transfer coefficients through finite bath experiments. *Ind Eng Chem Process Des Dev*. 1982;21:440–446.
11. Hulme R, Rosensweig RE, Ruthven DM. Binary and ternary equilibria for C_8 aromatics on K-Y faujasite. *Ind Eng Chem Res*. 1991; 30:752–760.
12. Hsiao HC, Yih SM, Li MH. Adsorption equilibrium of xylene isomers and p-diethylbenzene in the liquid phase on a Y zeolite. *Adsorption Sci Technol*. 1989;6:64–82.
13. Moya-Korchi V. *Étude de la contre-diffusion des xylènes dans des adsorbants zéolithiques de type Y*. Ph.D. thesis, L'Université Paris VI; 1995.
14. Minceva M, Rodrigues AE. Adsorption of xylenes on faujasite-type zeolite: equilibrium and kinetics in batch adsorber. *Chem Eng Res Design*. 2004;82:667–681.
15. Tournier H, Barreau A, Tavitian B, Le Roux D, Moise JC, Bellat JP, Paulin C. Adsorption equilibrium of xylene isomers and p-diethylbenzene on a prehydrated BaX zeolite. *Ind Eng Chem Res*. 2001; 40:5983–5990.

16. Pavone D, Hotier G. System approach modelling applied to the eluxyl process. *Revue de l'Institut Français du Pétrole*. 2000;55: 437–446.
17. Minceva M, Rodrigues AE. Influence of the transfer line dead volume on the performance of an industrial scale simulated moving bed for p-xylene separation. *Separat Sci Technol*. 2003;38:1463–1497.
18. Azevedo DCS, Neves SB, Ravagnani SP, Cavalcante Jr. CL, Rodrigues AE. *The Influence of Dead Zones on Simulated Moving Bed Units*. Proceedings of FOA6, ed. F. Meunier, pp 521–526. 6th Conf on Fundamentals of Adsorption. Elsevier, Paris; 1998.
19. Minceva M, Rodrigues AE. Modeling and simulation of a simulated moving bed for the separation of p-xylene. *Ind Eng Chem Res*. 2002;41:3454–3461.
20. Seader JD, Henley EJ. *Separation Process Principles*, 2nd Ed. New York: John Wiley & Sons, Inc; 2006:605.
21. Minceva M, Rodrigues AE. Two-level optimization of an existing SMB for p-xylene separation. *Comp Chem Eng*. 2005;29:2215–2228.
22. Kurup AS, Hidajat K, Ray AK. Optimal operation of an industrial-scale parex process for the recovery of p-xylene from a mixture of C8 aromatics. *Ind Eng Chem Res*. 2005;44:5703–5714.
23. *gPROMS v3 User Guide*. London: Process System Enterprise Ltd.; 2006.
24. Gomes PS, Minceva M, Rodrigues AE. Modelling, Simulation and Optimization of Cyclic Separation Processes. PSE Annual Meeting, London; April 25–26, 2006.
25. Storti G, Masi M, Carrá S, Morbidelli M. Modeling and design of simulated moving-bed adsorption separation units. *Chem Eng Sci*. 1989;44:1329–1345.
26. Azevedo DCS, Rodrigues AE. Design of a simulated moving bed in the presence of mass-transfer resistances. *AIChE J*. 1999;45:956–966.
27. Minceva M. Separation/Isomerization of Xylenes by Simulated Moving Bed Technology. Ph.D. thesis, University of Porto, Porto, Portugal; 2004.

Manuscript received July 25, 2006, and revision received Oct. 19, 2006.